Mapping of fluorescence anisotropy in living cells by ratio imaging

Application to cytoplasmic viscosity

James A. Dix and A. S. Verkman

Departments of Medicine and Physiology, Cardiovascular Research Institute, University of California, San Francisco, California 94143-0532

ABSTRACT Steady-state and time-resolved fluorescence properties of probes incorporated into living cells give information about the microenvironment near the probe. We have extended studies of spatially averaged fluorescence anisotropy (r) by using an epifluorescence microscope, equipped with excitation and emission polarizers and an image analysis system, to map r of nonoriented fluorophores incorporated into cultured cells. With this imaging system, r for reflected light or glycogen scattering solutions was > 0.98. Measurement of r over the range 0.01–0.35 for fluorophores in bulk solution and in thin capillary tubes placed side-by-side gave values equivalent to r measured by cuvette fluorometry. Cytoplasmic viscosity (η) in Madin-Darby canine kidney (MDCK) cells and Swiss 3T3 fibroblasts was examined from anisotropy images and time-resolved fluorescence decay of the cytoplasmic probes 2,7-bis-carboxyethyl-5 (and 6)-carboxy-fluorescein (BCECF) and indo-1. Nanosecond lifetimes and anisotropy decay were measured using a pulsed light source and gated detector interfaced to the epifluorescence microscope. Anisotropy images of BCECF in MDCK cells revealed two distinct regions of r: one from the cytoplasm ($r = 0.144 \pm 0.008$) and a second appearing at late times from the interstitial region ($r = 0.08 \pm 0.03$), representing BCECF trapped beneath the tight junctions. Anisotropy values, taken together with intracellular lifetimes and the calibration between r and η/τ_f for water/glycerol mixtures, gave η values of 10–13 cP at 23°C. These values assume little fluorophore binding to intracellular components and are therefore upper limits to cytoplasmic viscosity. These data establish a new methodology to map anisotropy in intact cells to examine the role of fluidity in cellular physiology.

INTRODUCTION

Fluorescence spectroscopy is a useful approach to examine the molecular motion of fluorophores in biological systems. Lipophilic fluorescent compounds incorporated into biological membranes have been used to correlate the physical state of cell membrane phospholipid with enzyme activity, the action of hormones, and alterations in membrane composition (Luly and Shinitzky, 1979; Hise et al., 1984; Illsley et al., 1987); hydrophilic compounds have been used to examine the viscous properties of cell cytoplasm (Burns, 1969; Luby-Phelps et al., 1988).

Time-resolved and steady-state fluorescence anisotropy (r) provides a detailed description of the rotational motion of fluorophores, which has been used to characterize the microviscosity of the environment surrounding the fluorophore. Because of technical and theoretical difficulties, r measurement has been applied almost exclusively to study cells and vesicles in suspension (e.g., Le Grimellec et al., 1982; Verkman and Ives, 1986; Verkman and Masur, 1988). There are, however, several classes of biological systems that are not amenable for study in suspension; examples of these are adherent cells whose properties may change when put in suspension, intact tissues having cellular heterogeneity, and macromolecular structures which cannot be isolated in sufficient quantity. In addition, all information about the distribution of r across a cell is lost when a spatially averaged measurement is performed.

We report here the application of quantitative imaging microscopy to obtain spatially resolved images of fluorescence anisotropy of fluid-phase fluorophores in the cytoplasm of two adherent cell lines, MDCK cells and Swiss 3T3 fibroblasts. In the accompanying paper (Fushimi et al., 1990), we report the application of anisotropy imaging to study r of probes incorporated into membranes, in which the fluorophore orientation is not random. Accurate images of r were calculated from a series of images taken through an epifluorescence microscope equipped with excitation and emission polarizers. The method was validated by imaging a series of thin capillary tubes containing fluorophores of known anisotropy and applied to measure anisotropy images of cytoplasm labeled with fluid-phase fluorescent probes. Time-resolved r and fluorescence lifetimes were measured by interfacing a nanosecond pulsed lifetime apparatus to the fluorescence microscope. Our results establish the methodology to obtain

Address correspondence to Dr. A. S. Verkman.

0006-3495/90/02/231/10 $2.00

accurate images of fluorescence anisotropy for studies of the biological role of cytoplasmic viscosity in monolayer cultured cells and cells in an intact epithelium.

METHODS

Chemicals

2,7-Bis-carboxyethyl-5[and 6]-carboxy-fluorescein (BCECF), indo-1, the acetomethoxy esters of BCECF and indo-1, (5[and 6]-carboxy-fluorescein) (CF), Pluronic F-127, and *N*-[3-sulfopropyl] acridinium (SPA) were obtained from Molecular Probes (Eugene, OR). 6-Methoxy-*N*-[3-sulfopropyl] quinolinium (SPQ) was synthesized by the method of Krapf et al. (1988). All other chemicals were obtained from Sigma Chemical Co. (St. Louis, MO).

Cell culture and fluorescence labeling

MDCK renal epithelial cells (ATCC CCL 34) and Swiss 3T3 fibroblasts (ATCC CCL 92) were obtained from the Cell Culture Facility of UCSF and used between passages 61 and 70 (MDCK) or 121 and 128 (3T3). Cells were grown at 37°C in 5% CO_2-95% air in Dulbecco's modified Eagle's medium supplemented with 10% fetal bovine serum, penicillin (100 U/ml), and streptomycin (100 μg/ml). Cells were grown to confluence on thin glass coverslips (18 mm diam).

Monolayer confluent cells on coverslips were washed three times with 2 ml of buffer and mounted in a cell perfusion chamber for continuous perfusion with specified buffers at constant temperature (Chao et al., 1989). Buffers used were Hank's balanced salt solution (HBSS) with 10 mM Hepes, pH 7.4 (for MDCK cells) or, in millimolar, 101 NaCl, 5 KCl, 2 $MgCl_2$, 2 $CaCl_2$, 5 D-glucose, 50 mannitol, and 5 Hepes/Tris, pH 7.4 (for 3T3 fibroblasts). Cells were labeled with 0.5–2 μM BCECF-AM or 1-5 μM indo-1-AM (containing 0.05 wt% Pluronic F-127) in the perfusion chamber. After 10 min (MDCK) or 15 min (3T3), external label was washed out and cells were perfused continuously with buffer. All experiments were carried out at ambient temperature (23–25°C).

Cuvette fluorometry

Steady-state r, lifetimes, and time-resolved r of fluorophores in bulk solution were measured by the phase-modulation method in a fluorometer equipped with Glan-Thompson calcite polarizers (model 48000; SLM Instruments Inc., Urbana, IL). The excitation light source was a 450-watt Xe arc lamp for steady-state r, or a HeCd laser (model 423ONB, 25 mW at 443 nm; Liconix, Sunnyvale, CA) for lifetimes and time-resolved r. BCECF fluorescence was excited at 475 nm (arc lamp) or 443 nm (laser), and detected through KV500 and OG515 cut-on filters. Indo-1 fluorescence was excited at 350 nm (arc lamp) or 325 nm (laser), and detected through KV408 and GG420 cut-on filters. The reference lifetime for indo-1 was POPOP in ethanol (1.35 ns); for BCECF, a glycogen scattering solution was used (0 ns). Background signal was <1% for all experiments.

IMAGE ANALYSIS

Apparatus

Fluorescently labeled cells were viewed with an inverted epifluorescence microscope (Nikon Diaphot-TMD-EF; Nippon Kogaku, Tokyo) which was modified to measure fluorescence anisotropy quantitatively (Fig. 1). All glass optics in the excitation path were replaced with fused silica. Fluorescence was excited by a 12-V, 50-W quartz-halogen lamp powered by an adjustable, stabilized DC power supply (Oriel, Stamford, CT). Excitation light was polarized in a horizontal plane with a polaroid film polarizer. Horizontal polarization was chosen for maximal reflection efficiency by the dichroic mirror. Excitation wavelength was selected with a six-cavity interference filter (bandwidth 10 nm; Omega Optical, Inc., Brattleboro, VT) and reflected into the perfusion chamber by a fused silica dichroic mirror (Omega Optical, Inc.). Objectives used were a 40× Fluor (Nikon, 1.3 NA, oil immersion, 0.17 mm working distance), 40× quartz (Leitz, 0.65 NA, glycerol immersion, 0.35 mm working distance), and 25× Fluotar (Leitz, 0.35 NA, air, 4 mm working distance).

Emitted light was filtered by a barrier filter; at low excitation wavelengths, a KV cut-on filter (Schott Glass, Duryea, PA) was used between the dichroic mirror and the barrier filter to reduce autofluorescence of the emission filter. Emitted light passed through a rotatable film polarizer to analyze fluorescence depolarization. Images taken with different polarizer orientations were superimposable to within one pixel at 100×. The image was focused onto a variable gain, microchannel plate image intensifier (Videoscope International, Washington, DC), and imaged with a solid-state CCD camera (Cohu Inc., San Diego, CA) operating at fixed gain.

The output of the CCD camera was digitized with a frame grabber (model DT2861; Data Translation, Natick, MA) in a 80286 computer with 80287 math coprocessor (Rose Hill, Scotts Valley, CA). An auxiliary processing board (model DT2858; Data Translation) was used to speed frame processing. 512 × 512 × 8 bit images were stored on a dedicated 110-MB hard disk drive and archived with a 60-MB streaming tape drive (Everex, Fremont, CA). The output of the CCD camera or the frame processor could also be stored on a Super-VHS video cassette recorder (Mitsubishi, Cypress, CA). Data acquisition and analysis software was written in Microsoft Fortran 4.0 using the Fortran subroutine library purchased from Data Translation.

Polarizer alignment

Polarizers were aligned before each set of experiments for accurate measurement of anisotropy values. The excitation polarizer was aligned

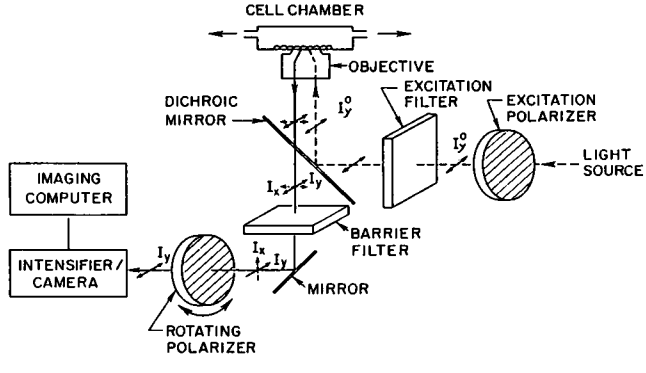

FIGURE 1 Fluorescence anisotropy imaging apparatus. See Methods for a description of the apparatus. The excitation polarizer is aligned so that light is horizontally polarized (y-axis). The emission polarizer is rotated to be parallel to the y-axis (for measurement of $I_\parallel$) and to be parallel to the x-axis (for measurement of $I_\perp$).

to a horizontal position by maximizing detected light in the absence of an emission polarizer, making use of the polarization characteristics of the dichroic mirror. To align the emission polarizer, the dichroic mirror was replaced with a partially silvered mirror and the perfusion chamber was replaced with a front surface mirror; the emission polarizer was rotated until a minimum in reflected light intensity was obtained. Alignment was checked periodically by measuring the anisotropy of reflected light or of light scattered from a glycogen solution placed in the perfusion chamber. Anisotropy values > 0.98 were routinely obtained, and were invariant over excitation wavelengths 350–500 nm.

Background correction

Background intensities were obtained by mounting nonlabeled cells in the perfusion chamber, then measuring the signal intensity as a function of polarizer orientation, lamp voltage, intensifier gain, and excitation wavelength. For a given set of experimental conditions, different cell samples gave background signals that varied by <5%. The background signal was found to be spatially uniform for studies reported here. The maximum background signal from the cells was 9% of the full gray scale; at the weakest fluorescence signal measured in the experiments reported here, this background signal represented 12% of the total light intensity. The background signal at the appropriate light intensity, intensifier gain, excitation wavelength, and polarizer orientation was subtracted from measured fluorescence intensity.

System calibration and anisotropy calculation

The flatness of the imaged field was determined to be better than 0.5% based on the image of a uniform solution of CF. The linearity of the response of the anisotropy imaging system was determined by imaging solutions of CF or SPA of varying concentration in the perfusion chamber (Fig. 2). At relatively high signal intensities, in which the image histograms were narrow, a linear response is observed (Fig. 2, *top*). However, at lower light intensity and at maximal system gain, the response began to saturate as the leading tail of the broad image histogram exceeds the limit of the A/D converter (Fig. 2, *bottom*). When necessary, saturation effects were taken into account by relating the measured fluorescence intensity, $F_{i,j}$, to the true fluorescence intensity at pixel i, j, $I_{i,j}$ (which is proportional to fluorophore concentration in these experiments), by an empirical equation,

$$F_{i,j} = a_0 + a_1(I_{i,j}) + a_2(I_{i,j})^2, \quad (1)$$

where a separate set of a_i factors were required for parallel and perpendicular orientations of the emission polarizer. The correction becomes increasingly important at higher system gain, where optical noise broadens the histogram of gray scale levels. As shown in Fig. 2, this correction was <2% even at high intensifier gain when signal levels were maintained within the lower half of the 0–255 gray scale (<128).

To correct for the polarization dependence of detector sensitivity, two methods were used which gave the same results. In the first method, the perfusion chamber was removed, and unpolarized light was passed through an interference filter, the dichroic mirror and the emission polarizer, and detected by the intensifier/camera. The differential detector sensitivity (G-factor) was determined from the ratio of corrected intensities calculated for perpendicular and parallel orientations of the emission polarizer. In the second method, the fluorescence anisotropy of a fluorophore in aqueous solutions having near zero anisotropy

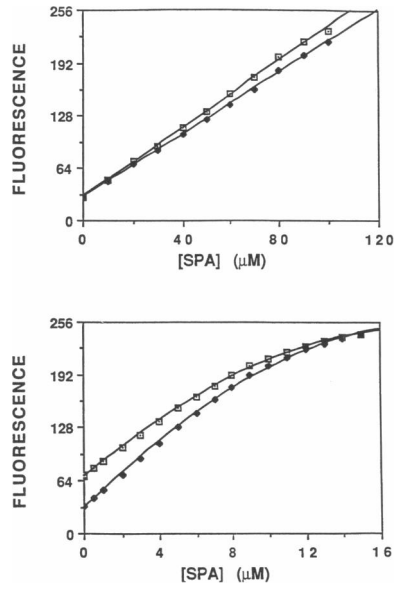

FIGURE 2 Anisotropy imaging system response. Aqueous solutions of SPA were passed through the perfusion chamber and images with polarizers parallel (□) and perpendicular (◆) were acquired at constant gain. The images were obtained through the 100× oil-immersion objective focused just above the coverslip. Excitation was at 380 ± 5 nm with a 400-nm dichroic mirror; emitted light was filtered by KV408 and GG420 cut-on filters. The abscissa gives the average intensity/pixel of a 100-frame average at each concentration; the data in the figure were not corrected for background signal. The upper figure gives data taken with [SPA] = 0–120 μM, where the system gain was near half-maximal. The lower figure gives data taken with [SPA] = 0–16 μM, where the system gain was near maximal. Curves are the fit of a quadratic equation, $y = a_0 + a_1 \times a_2x^2$, to the data. For the upper figure, fitted parameters were a_0 = 29.8 and 27.9, a_1 = 1.89 and 2.22, $a_2 = 8.83 \times 10^{-6}$ and -1.59×10^{-3} for parallel and perpendicular, respectively; for the lower figure, fitted parameters were a_0 = 68.6 and 30.9, a_1 = 19.5 and 22.6, a_2 = −0.508 and −0.561 for parallel and perpendicular, respectively. At the SPA concentrations used, inner filter and self-quenching effects were absent.

was measured, in which detected light intensity should be nearly independent of the orientation of the emission polarizer. The G-factor was calculated from the relation

$$G = (I_{\parallel i,j}/I_{\perp i,j})(1 - r_m)/(1 + 2r_m), \quad (2)$$

where r_m is the known near zero anisotropy, and $I_{\parallel i,j}$ and $I_{\perp i,j}$ are the corrected intensities at pixel i, j measured with parallel and perpendicular orientations of the emission polarizer, respectively. The value of G depended on emission wavelength (e.g., 0.835 ± 0.020 [SD, n = 16] at 430 nm; 0.737 ± 0.016 [SD, n = 27] at 530 nm) but was independent of intensifier gain, light intensity, and pixel location. The G-factor was determined at the beginning and end of every set of experiments.

The corrected anisotropy of pixel i,j (r_{ij}) was calculated as

$$r_{ij} = (1 - G \cdot I_{\perp i,j}/I_{\parallel i,j})/(1 + 2G \cdot I_{\perp i,j}/I_{\parallel i,j}). \quad (3)$$

The anisotropy image was displayed using an eight-bit gray scale or by pseudocolor.

Time-resolved fluorescence microscopy

Fluorescence lifetimes and anisotropy decay were measured by interfacing a nanosecond pulsed lifetime instrument (model LS-1; PTI, London/Ontario, Canada) to the epifluorescence microscope. Time-dependent fluorescence was measured by replacing the quartz-halogen light source and intensifier/camera in Fig. 1 by the nanosecond flashlamp and gated photomultiplier from the PTI instrument. Data acquisition for this instrument is based not on time-correlated photon counting, but on measurement of the integrated photomultiplier current under conditions when the photomultiplier is gated on for 0.1-ns intervals at varying times after the upstroke of the flash. Greater excitation intensities could be employed in this method to speed data acquisition from labile cell samples. For anisotropy decay, the flashlamp was filled with N_2 gas; for lifetime determination, the polarizers were removed and the flashlamp filled with D_2 gas. The flashlamp operated at 4–6 kV at a repetition rate of 25 kHz. Typically, 200 data points, each data point representing 25 A/D conversions, were acquired for each 15-s time scan.

The flashlamp profile at the excitation wavelength was determined by replacing the cell perfusion chamber with a front-surfaced mirror and removing the barrier filter. The flashlamp profile was measured periodically throughout the course of an experiment and usually was constant to within one data point. When necessary, data were time-shifted using the flashlamp profile as a reference. In a typical experiment, 20 scans, obtained in groups of 5–10 interspersed with flashlamp profile data, were averaged. For anisotropy decay experiments, the *G*-factor was determined from the multiplicative value necessary to equalize the parallel and perpendicular intensities of SPQ and SPA in water; *G*-values determined in this way were identical to those determined from steady-state anisotropy measurements. Data were analyzed to calculate lifetime or anisotropy decay parameters using software purchased from PTI.

For experiments with indo-1, background scans were obtained from cells before labeling. Background signal was 20–30% of the total signal intensity and was subtracted. Separate background scans were obtained for parallel and perpendicular polarizer orientations for anisotropy decay experiments. Background signal was <2% for the BCECF experiments.

RESULTS

Model studies

To validate the accuracy of the imaging system for measurement of fluorescence anisotropy, images were obtained of CF in a series of bulk glycerol/water mixtures. Fig. 3 shows the relationship between *r* measured by cuvette fluorimetry and by imaging microscopy. These results show that *r* can be measured accurately and with good precision by the imaging system.

To demonstrate the ability to measure fluorescence anisotropy with spatial resolution, thin capillary tubes filled with CF in varying glycerol/water mixtures were imaged with the emission polarizer oriented parallel (Fig. 4, *left*) and perpendicular (Fig. 4, *center*). The greatest difference in fluorescence intensity measured using the two polarizer orientations, and thus the highest *r*, was

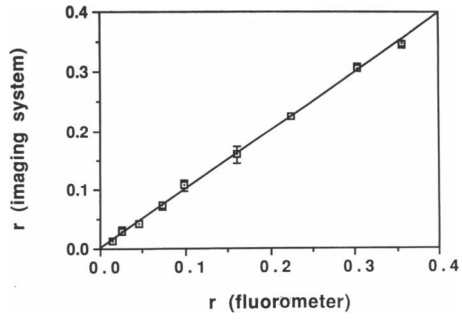

FIGURE 3 Comparison of fluorescence anisotropy determined by cuvette fluorometry and by the imaging system. The fluorescence anisotropy of a solution of 1 μM CF in glycerol/water was determined using either a fluorometer (r_{fl}, abscissa) or the imaging system (r_{im}, ordinate) using the 40× Fluor objective. *y*-axis error bars represent the standard deviation of three determinations of r_{im}; the errors in r_{fl} were <0.0003 and are smaller than the size of the points. The line of identity is plotted. Anisotropy values obtained using a 4× objective did not differ significantly from data shown. High NA objective depolarization was not observed in studies of *r* in bulk solutions, probably because the majority of measured signal arises from out-of-focus fluorescence entering the objective at shallow angles.

from the capillary tube on the bottom, which contained the most viscous solvent (99% glycerol). An anisotropy image of the capillary tubes (Fig. 4, *right*) shows that regions of an image can be distinguished based on fluorescence anisotropy. The measured *r* were 0.127 ± 0.009 (*top tube*), 0.218 ± 0.011 (*middle tube*), and 0.330 ± 0.012 (*bottom tube*); corresponding *r* determined from the same samples measured by cuvette fluorometry were 0.132, 0.225, and 0.338 ($SD < 0.001$), respectively. Multiple determinations of *r* made by imaging the same sample agreed to within 0.002; reported errors were determined by propagating the error in *G* and the background correction into *r*. The anisotropy image within a tube was uniform; the standard deviations of *r* values for pixels within a tube were 0.009 (*top tube*), 0.012 (*middle tube*), and 0.012 (*bottom tube*).

To validate the accuracy of the lifetime microscope, lifetime decays were obtained from the chloride-sensitive fluorophore, SPQ, for chloride concentrations in the range 0–150 mM. SPQ is quenched by chloride by a collisional mechanism with a Stern-Volmer quenching constant of 118 M^{-1} (Illsley and Verkman, 1987). The lifetime of SPQ in water at [Cl] = 0 determined in the lifetime microscope was 26 ± 1 ns, identical to that reported using phase/modulation fluorometry. The lifetime decreased hyperbolically with [Cl], reaching 2 ns at [Cl] = 150 mM; the Stern-Volmer quenching constant was 115 ± 6 M^{-1} (data not shown). These data indicate that accurate lifetime data can be obtained by fluorescence microscopy.

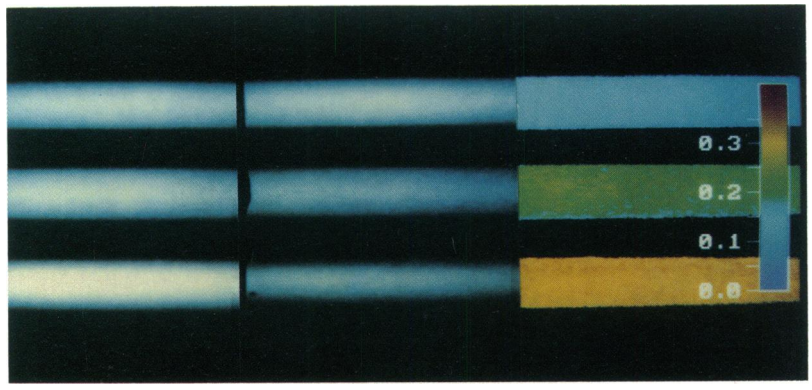

FIGURE 4 Spatially resolved anisotropy image of capillary tubes filled with 10 μM CF in water/glycerol (wt/wt) mixtures of 40:60 (*top tube*), 20:80 (*middle tube*), or 1:99 (*bottom tube*). Capillaries were viewed with a 4× (NA 0.10) objective. The three tubes were imaged with polarizers oriented parallel (*left*) or perpendicular (*middle*). The pseudocolored anisotropy images of the tubes is given at the right with color bar legend.

Steady-state anisotropy of cytoplasmic fluorophores

To estimate cytoplasmic viscosity, r for BCECF and indo-1 in MDCK cells and Swiss 3T3 fibroblasts was measured. BCECF and indo-1 were chosen because they are fluid-phase cytoplasmic markers that are available as cell-permeable acetoxymethyl esters. The fluorophore BCECF has been used extensively as a probe of intracellular pH in intact cells (Rink et al., 1982). BCECF is localized in the cell cytoplasm and is thought not to bind significantly to cellular proteins. Indo-1 has been used as a probe of intracellular calcium (Grynkiewicz et al., 1985).

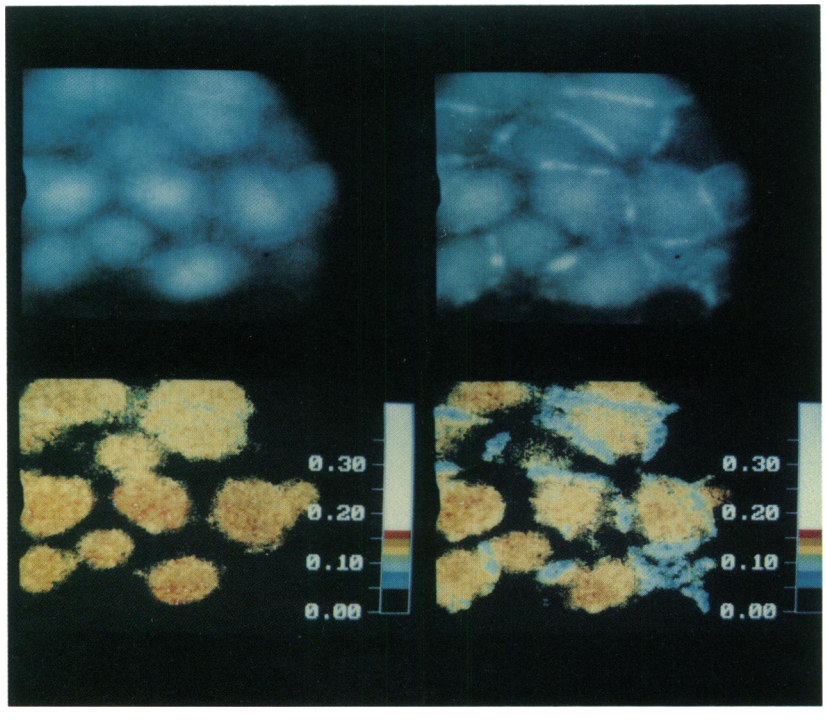

FIGURE 5 BCECF labeling of MDCK cells. MDCK cells grown to confluence on round glass coverslips were mounted in the perfusion chamber, perfused with 5 μM BCECF-AM for 10 min, then perfused continuously with HBSS at 23°C. The fluorescence images 10 and 40 min after the start of the BCECF-AM perfusion are given in the upper photos; the anisotropy image of the same fields are given in the lower photos.

Fig. 5, upper left, shows an image of BCECF-labeled MDCK cells 10 min after washing BCECF-AM from cells. Under these conditions there is a fairly uniform cytoplasmic distribution without bright spots. The pseudocolored anisotropy image of the same field is shown in Fig. 5, lower left; similar images were obtained for BCECF-labeled Swiss 3T3 fibroblasts (not shown). The anisotropy images were calculated pixel by pixel by Eq. 3. For both cell lines, BCECF anisotropy was fairly uniform across a cell, with some nonuniformity that may be due to dye binding; the standard deviation of r within a cell was 0.006. The spatially averaged values for r (Table 1) were similar in both cell lines.

Fig. 5, upper right, shows that 40 min after exposure to BCECF-AM, additional BCECF fluorescence is present in the region between the cells; BCECF-labeled 3T3 fibroblasts did not show this additional fluorescence. The intercellular fluorescence, not reported in previous BCECF/MDCK studies (Goldfarb and Nord, 1987; Selvaggio et al., 1986), may represent binding to plasma membrane proteins, or leakage of BCECF from the interior of the cells into the interstitial space beneath the epithelial tight junction. An anisotropy image (Fig. 5, *lower right*) of the field indicates that the fluorescence appearing after 40 min is of lower anisotropy ($r = 0.08 \pm 0.03$) and probably represents BCECF that has leaked or been transported from the cytoplasm and has become trapped beneath the tight junction in the intercellular space. The fraction of total fluorescence in the intercellular compartment having low r increased progressively with time after washing of BCECF-AM; the anisotropy of BCECF remaining within the cytoplasm did not change. These results demonstrate the ability to measure spatially resolved r of BCECF in different environments.

Fluorescence and anisotropy images of indo-1 in MDCK cells and Swiss 3T3 fibroblasts were obtained. Anisotropy was spatially uniform across the cell with standard deviation 0.010 (MDCK cells) and 0.007 (fibroblasts). There was no significant difference in r between cell lines (Table 1).

There are several potential artifacts in the determination of r by microscopy. To show that the cell monolayer did not introduce depolarization, MDCK cells were mounted in the perfusion chamber and perfused with 5 μM SPA in buffer or 6 μM CF in buffer/glycerol (1:1). Steady-state r was unaffected by the presence of the cell monolayer between the objective and solutions containing the impermeant fluorophores.

Polarization artifacts can be caused by objectives with high numerical aperture (Axelrod, 1979; 1989). The magnitude of this effect depends upon several factors, including the objective NA, refractive index of the media adjacent to the objective, the spatial distribution of fluorophores, and the time-resolved rotational motion of the fluorophore. A theoretical correction of r for these effects would be extremely difficult. To examine experimentally whether there was significant objective depolarization under conditions of these experiments, we compared r measured with 40× 1.3 NA, 40× 0.65 NA and 25× 0.35 NA objectives. The results (Table 2) indicate no significant effect of numerical aperture on measured r in these studies. Under some conditions with use of highly hindered membrane-bound fluorophores (see accompanying manuscript), high NA effects were observable.

TABLE 1 Anisotropy and lifetime of BCECF and indo-1 in MDCK and Swiss 3T3 fibroblasts*

Probe	Cell	r	τ_f
			ns
BCECF	MDCK	0.144 ± 0.008 (n = 58)	3.76 ± 0.19 (n = 4)
BCECF	Swiss 3T3	0.141 ± 0.010 (n = 66)	3.84 ± 0.03 (n = 4)
indo-1	MDCK	0.26 ± 0.02 (n = 26)	1.92 ± 0.11 (n = 4)
indo-1	Swiss 3T3	0.24 ± 0.03 (n = 70)	2.03 ± 0.22 (n = 4)
BCECF	Water	0.0235 ± 0.0001	3.09 ± 0.03
indo-1	Water	0.0703 ± 0.0001	1.81 ± 0.08

*Lifetimes (τ_f) and r (mean ± SD) in cells were measured in the microscope; those in water were measured in the fluorometer. Ground-state heterogeneity analysis showed that a single lifetime described the data for probes in cells and for BCECF in water; for indo-1 in water, a small (1–2%) component of long lifetime (50–100 ns) was detected.

Time-resolved fluorescence microscopy

Steady-state r depends upon fluorescence lifetime and the detailed rotational motion of the fluorophore in its local environment. To interpret r values in terms of effective cytoplasmic viscosity, fluorescence lifetimes of BCECF and indo-1 were determined in MDCK cells and Swiss 3T3 fibroblasts using a nanosecond pulsed lifetime apparatus interfaced to the microscope. Typical data are given in Fig. 6; lifetimes are given in Table 1. The lifetime of probes in cytoplasm was 10–20% greater than in water; there was no significant difference between cell lines. The similarity of probe lifetimes in cytoplasm and in water

TABLE 2 Effect of objective NA on measured anisotropy in Swiss 3T3 fibroblasts

Objective	NA	r(BCECF)	r(indo-1)
Nikon 40×, oil	1.3	0.132 ± 0.007	0.24 ± 0.03
Leitz 40×, glycerol	0.65	0.131 ± 0.017	0.26 ± 0.02
Leitz 25×, air	0.35	0.134 ± 0.008	—*

*Signal intensity was too weak to obtain reliable data.

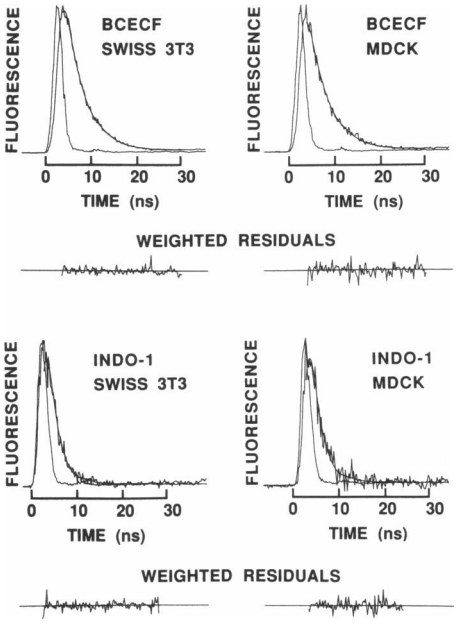

FIGURE 6 Fluorescence lifetimes of BCECF and indo-1 in cells. Cells were mounted and labeled; lifetime data were acquired as described in Methods. Fluorescence was measured over a single cell. The figures display the flashlamp profile (*narrow curve*), fluorescence decay (*wide curve*), and the fit for single exponential intensity decay (*smooth line*) through the data. Fitted lifetimes and chi-squared values were 3.86 ± 0.04 and 0.72 (BCECF, 3T3), 3.88 ± 0.06 and 0.91 (BCECF, MDCK), 1.93 ± 0.05 and 1.88 (indo-1, 3T3), and 1.94 ± 0.12 and 1.47 (indo-1, MDCK). The weighted residuals from the fit are given below each figure. Chi-squared values were not improved significantly by inclusion of a second lifetime.

suggests that probe self-quenching, and hence concentration-dependent depolarization, does not occur.

To relate steady-state r to hydrodynamic viscosity, r was "calibrated" as a function of viscosity (η) and lifetime (τ_f) for indo-1 and BCECF in mixtures of water/glycerol by cuvette fluorometry. The data fit well to a saturable function of η/τ_f (Fig. 7), consistent with predictions from the Perrin equation for fluorophore rotation in bulk solutions,

$$r = r_o/(1 + \tau_f/\tau_c) = r_o(\eta/\tau_f)/[(\eta/\tau_f) + (kT/V_h)], \quad (4)$$

where τ_c is the rotational correlation time and V_h is the hydrated fluorophore volume. The data suggest that the indo-1 hydrated volume, as measured by steady-state r in water/glycerol solutions, is twice that of BCECF.

In using Eq. 4 to compare aqueous and cytoplasmic viscosities, it has been assumed that probe rotational motion is similar in the two environments. This is an unproven assumption that has not been tested in previous studies of intracellular viscosity. We used two approaches to examine whether probe rotational motion in cells is similar to that in bulk solution of equivalent effective viscosity. The first approach was to compare measured viscosities using two very different fluorophores and cell types (see below). The second approach was to compare the time-resolved anisotropy decays of indo-1 and BCECF in cells to the decays in water and water/glycerol (1:1, 6 cP). Because of rapid probe rotation and the finite width of the N_2 flash lamp, rotational correlation times were not well determined but were generally <2 ns. Apparent limiting anisotropies (r_∞) obtained from a fit of a single hindered rotator model to decay data for BCECF were 0.06 ± 0.04 (Swiss 3T3) and 0.09 ± 0.05 (MDCK); for indo-1, r_∞ were 0.18 ± 0.10 (Swiss 3T3) and 0.09 ± 0.05 (MDCK). Corresponding values for BCECF in aqueous solution were 0.02 ± 0.02 (water) and 0.09 ± 0.03 (water/glycerol); for indo-1, r_∞ values were 0.07 ± 0.03 (water) and 0.17 ± 0.09 (water/glycerol). These values suggest that probe rotational motion is significantly hindered in cytoplasm and viscous aqueous solutions, however, improved measurements of probe nanosecond rotation within the cell cytoplasm are required to determine the extent of binding of the probe to intracellular components (see Discussion). If fluorophore motion is highly hindered and fluorophore orientation nonrandom, special methods must be used to measure r as developed in the accompanying paper (Fushimi et al., 1990).

If it is assumed that fluorophore rotational characteristics in cells are similar to those in water/glycerol, an effective cytoplasmic viscosity can be estimated from the data in Fig. 7; these values are given in Table 3. If there were significant binding of the fluorophore to intracellular components, the estimated viscosity values represent an upper limit to the fluid-phase cytoplasmic viscosity.

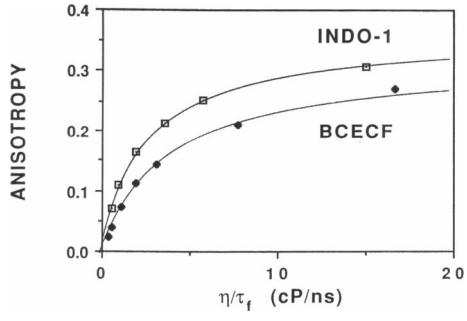

FIGURE 7 Steady-state r for indo-1 and BCECF in water/glycerol mixtures. Probes at 5 μM were placed in water/glycerol mixtures ranging from 1:0 to 3:22 (wt/wt), giving viscosities of 1.0–147 cP (CRC Handbook). Steady-state r was determined in a fluorometer. The fitted lines are a fit of a saturable, hyperbolic function to the data; the half-saturation values are 5.4 cP/ns for BCECF and 2.7 cP/ns for indo-1.

TABLE 3 **Cytoplasmic viscosities**

Cell	Probe	Viscosity*
		cP
MDCK	BCECF	13 ± 1
MDCK	indo-1	12 ± 3
Swiss 3T3	BCECF	13 ± 1
Swiss 3T3	indo-1	10 ± 3

*These are upper limits to cytoplasmic viscosity at 23°C assuming no binding of fluorophores to cell cytoplasmic components.

DISCUSSION

The results presented here demonstrate the feasibility of imaging fluorescence anisotropy in intact cells and of measuring cytoplasmic viscosity in adherent cells. Control experiments with fluorophores in bulk solution indicate that measurement of r with the anisotropy imaging system is equivalent to measurement of r with a fluorometer. Anisotropy can be measured reproducibly to within 0.002 and to an accuracy of better than 5%. Experiments with capillary tubes filled with fluorophores in solutions of differing viscosities showed that r can be resolved spatially within a microscope field. Anisotropy measured in different parts of the field are equivalent to those measured in a fluorometer. The presence of a cell monolayer did not cause measurable fluorescence depolarization. The similarity of cell anisotropy measured with objectives having widely different NA showed that objective depolarization effects were very small in these studies. If the measured r had decreased with increasing NA, then it would have been necessary to choose a low NA objective in which r was independent of NA. If use of a low NA objective were impossible because of low signal intensities, then an empirical correction factor or a detailed mathematical analysis (Axelrod, 1989) would be required.

The anisotropy imaging system was used to investigate cytoplasmic viscosity of MDCK cells and Swiss 3T3 fibroblasts by measuring r of the intracellular probes, BCECF and indo-1. Although steady-state fluorescence anisotropy has been used previously to estimate cytoplasmic viscosity of cells in suspension (e.g., Lindmo and Steen, 1977; Hashimoto and Shinozaki, 1988; Burns, 1969), the present work represents the first application of r to estimate cytoplasmic viscosity of adherent cells. To interpret steady-state r values quantitatively, a nanosecond pulsed fluorescence microscope was constructed to measure lifetimes and time-resolved anisotropy of fluorophores in cells.

Time-resolved fluorescence decay revealed similar fluorophore lifetimes in cytoplasm and in water or water/glycerol mixtures. However there were differences in probe rotational characteristics (as measured by an apparent r_∞ values) in the two environments. Both indo-1 and BCECF are planar molecules whose excitation and emission dipoles lie within the plane, and would be expected a priori to have anisotropic rotation. If out-of-plane depolarizing rotations were much slower than inplane rotations, then the fluorophore would, over a restricted time range, exhibit apparent hindered rotation and nonzero r_∞ when depolarization data are interpreted in terms of an isotropic hindered rotator model. We found similar anisotropy decays in viscous aqueous solutions and in cytoplasm, so that calibrations of r vs. η/τ_f performed in aqueous solutions were used to approximate η/τ_f in cytoplasm; measurement of intracellular τ_f can then be used to estimate cytoplasmic viscosity. However, because of the inability to measure accurately the anisotropy decay of the fluorophores in the cytoplasm, particularly rotational correlation times, it is not possible to rule out fluorophore binding to intracellular components. If binding occurs, the apparent viscosity values would be greater than the true fluid-phase viscosity. Therefore, our viscosity values should be regarded as upper limits to the true viscosity.

The cytoplasmic viscosity of Swiss 3T3 fibroblasts determined in this study, 10–13 cP at 23°C (8–10 cP at 37°C assuming an activation energy of 3.7 kcal/mol [Lepock et al., 1983]) is similar to viscosities reported in several cells lines in suspension examined by fluorescence polarization methods (6–13 cP at 37°C; Burns, 1969; Lindmo and Steen, 1977). However, our value is somewhat greater than that measured by fluorescence recovery after photobleaching of fluorescently labeled dextrans (4 cP at 37°C; Luby-Phelps et al., 1986), and greater than values reported for rotation of small molecules in cytoplasm measured by electron spin resonance (3–6 cP; Lepock et al., 1983; Mastro et al., 1984).

The cytoplasm is thought to consist of a network of microtubules, F-actin, and intermediate filaments that form a cytoplasmic "mesh" (Porter, 1984); for Swiss 3T3 fibroblasts, the mesh size has been estimated to be in the range 20–40 nm (Luby-Phelps et al., 1986). The hydrated volumes of BCECF and indo-1 obtained from the Perrin equation (Fig. 7) give a hydrodynamic radii on the order of 0.6–0.7 nm for these probes, much smaller than the mesh size. Therefore, the cytoplasmic filamentous network would not be expected to strongly influence probe rotation. As discussed above, binding of fluorophore to cytoplasmic components would cause an elevation in r above that predicted for a freely rotating fluorophore; additional measurements of anisotropy decay of the fluid-phase fluorophores are required to quantitate the degree of binding. Therefore, the higher viscosities that have been determined from fluorescence measurements may be due to significant fluorophore binding within the cell.

Because anisotropy is calculated for individual pixels, the theoretical resolution of anisotropy mapping should be that of the epifluorescence light microscope. In a sample with heterogeneous anisotropies, out-of-focus fluorescence information would limit the spatial resolution (see Appendix of Fushimi et al., 1990, accompanying manuscript); however, optical sectioning techniques would restore full resolution. It should be noted that the optics of a confocal microscope do not interfere with polarization measurements, making it possible to map anisotropy in submicrometer optical sections. Another potential concern in the mapping of subcellular anisotropy is depolarization due to scattering of excitation or emission light. This problem should be minimal for thin samples, however, it should be evaluated for thick, turbid samples containing fluorophores with low molar absorbance. Finally, it should be emphasized that high numerical aperature depolarization could result in artifactually low anisotropy values, particularly for slowly rotating fluorophores with high anisotropy.

In summary, the results reported here establish the methodology to image fluorescence anisotropy and to obtain time-resolved fluorescence data in single cells by fluorescence microscopy. There are several important applications for anisotropy mapping by quantitative imaging microscopy. In contrast to other reported methods, it is possible to measure cytoplasmic viscosity in cells grown on substrate, in single cells, and in localized regions of single cells. Spatial resolution of r was important to identify the origin of the redistribution of BCECF fluorescence seen 40 min after loading. r can be measured in the presence of a large background signal outside of the region of interest. In experiments with BCECF-labeled MDCK cells, cytoplasmic r was measured in the presence of a large signal from interstitial BCECF; measurement of a spatially averaged r would lead to a serious underestimate of true cytoplasmic r. Anisotropy imaging is essential with cellular heterogeneity, as present in most epithelial systems, and even in a pure culture of cells that are not synchronized with respect to the cell cycle. Finally, the ability to measure and to detect small changes in anisotropy in selected membrane or cytoplasmic regions of a single living cell provides an approach to examine the cellular regulation of fluidity and the role of fluidity in the modulation of cellular functions.

We thank Mary Sellers for help with cell culture.

This work was supported by grants DK35124, DK39354, and HL43268 from the National Institutes of Health, a grant-in-aid from the American Heart Association, and a grant from the National Cystic Fibrosis Foundation. A. S. Verkman is an Established Investigator of the American Heart Association.

Received for publication 25 May 1989 and in final form 22 September 1989

REFERENCES

Axelrod, D. 1979. Carbocyanine dye orientation in red cell membrane studied by microscopic fluorescence polarization. *Biophys. J.* 26:557–574.

Axelrod, D. 1989. Fluorescence polarization microscopy. *Methods Cell Biol.* 30:333–352.

Burns, V. W. 1969. Measurement of viscosity in living cells by a fluorescence method. *Biochem. Biophys. Res. Commun.* 37:1008–1014.

Chao, A. C., J. A. Dix, M. C. Sellers, and A. S. Verkman. 1989. Fluorescence measurement of chloride transport in monolayer cultured cells: mechanisms of chloride transport in fibroblasts. *Biophys. J.* 56:1071–1081.

Fushimi, K., J. A. Dix, and A. S. Verkman. 1990. Cell membrane fluidity in the intact kidney proximal tubule measured by orientation-independent fluorescence anisotropy imaging. *Biophys. J.* 57:241–254.

Goldfarb, D., and E. P. Nord. 1987. Asymmetric affinity of Na^+-H^+ antiporter for Na^+ at the cytoplasmic versus external transport site. *Am. J. Physiol.* 253:F959–F968.

Grynkiewicz, G., M. Poenie, and R. Y. Tsien. 1985. A new generation of Ca^{2+} indicators with greatly improved fluorescence properties. *J. Biol. Chem.* 260:3440–3450.

Hashimoto, Y., and N. Shinozaki. 1988. Measurement of cytoplasmic viscosity by fluorescence polarization in phytohemagglutinin-stimulated and unstimulated human peripheral lymphocytes. *J. Histochem. Cytochem.* 36:609–613.

Hise, M. K., M. Mantulin, and E. J. Weinman. 1984. Fluidity and composition of brush border and basolateral membranes from rat kidney. *Am. J. Physiol.* 247:F434–F439.

Illsley, N. P., and A. S. Verkman. 1987. Membrane chloride transport measured using a chloride-sensitive fluorescent indicator. *Biochemistry.*26:1215–1219.

Illsley, N. P., H. Y. Lin, and A. S. Verkman. 1987. Lipid domain structure correlated with membrane protein function in placental microvillus vesicles. *Biochemistry.* 26:446–454.

Krapf, R., N. P. Illsley, H. C. Tseng, and A. S. Verkman. 1988. Structure-activity relationships of chloride-sensitive fluorescent indicators for biological application. *Anal. Biochem.* 169:142–150.

Le Grimellec, C., M.-C. Giocondi, B. Carriere, S. Carriere, and J. Cardinal. 1982. Membrane fluidity and enzyme activities in brush border and basolateral membranes of the dog kidney. *Am. J. Physiol.* 242:F246–F253.

Lepock, J. R., K.-H. Cheng, S. D. Campbell, and J. Kruuv. 1983. Rotational diffusion of tempone in the cytoplasm of Chinese hamster lung cells. *Biophys. J.* 44:405–412.

Lindmo, T., and H. B. Steen. 1977. Flow cytometric measurement of the polarization of fluorescence from intracellular fluorescein in mammalian cells. *Biophys. J.* 18:173–187.

Luby-Phelps, K., F. Lanni, and D. L. Taylor. 1988. The submicroscopic properties of cytoplasm as a determinant of cellular function. *Annu. Rev. Biophys. Biophys. Chem.* 17:369–396.

Luby-Phelps, K., D. L. Taylor, and F. Lanni. 1986. Probing the structure of cytoplasm. *J. Cell Biol.* 102:2015–2022.

Luly, P., and M. Shinitzky. 1979. Gross structural changes in isolated liver cell plasma membranes upon binding of insulin. *Biochemistry.*18:445–452.

Mastro, A. M., M. A. Babich, W. D. Taylor, and A. D. Keith. 1984.

Diffusion of a small molecule in the cytoplasm of mammalian cells. *Proc. Natl. Acad. Sci. USA.* 81:3414–3418.

Porter, K. R. 1984. The cytomatrix: a short history of its study. *J. Cell. Biol.* 99:3s–12s.

Rink, T. J., R. Y. Tsien, and T. Pozzan. 1982. Cytoplasmic pH and free Mg^{++} in lymphocytes. *J. Cell Biol.* 95:185–196.

Selvaggio, A. M., J. H. Schwartz, H. H. Bengele, and E. A. Alexander. 1986. Kinetics of the Na^{+}-H^{+} antiporter as assessed by the change in intracellular pH in MDCK cells. *Am. J. Physiol.* 251:C558–562.

Verkman, A. S., and H. E. Ives. 1986. Water transport and fluidity of renal basolateral membranes. *Am. J. Physiol.* 250:F633–F643.

Verkman, A. S., and S. K. Masur. 1988. Very low osmotic water permeability and membrane fluidity in isolated toad bladder granules. *J. Membr. Biol.*104:241–251.